Geometrical Preference of Ruthenium Oxidation States: Metal Redox and Isomerisation of $[Ru(S_2CNEt_2)_2(PPh_3)_2]^{0,+}$ †

Mahua Menon, Amitava Pramanik, Nilkamal Bag and Animesh Chakravorty*
Department of Inorganic Chemistry, Indian Association for the Cultivation of Science, Calcutta 700 032, India

Reaction of $Na[S_2CNEt_2]$ with $[Ru(PPh_3)_3Cl_2]$ afforded *cis*-$[RuL_2(PPh_3)_2]$ (L = S_2CNEt_2), which upon oxidation by cerium(IV) furnished *trans*-$[RuL_2(PPh_3)_2]^+$, isolated as its PF_6^- salt. Both complexes are obtained in nearly quantitative yields. The trivalent complex displays one-electron paramagnetism and a rhombic frozen-solution EPR spectrum which has been analysed affording axial and rhombic distortion parameters of ≈8000 and ≈1700 cm^{-1} respectively. A ligand-field transition within the Kramers doublets is observed at 6450 cm^{-1}, the predicted value being ≈7000 cm^{-1}. Variable-temperature (253–303 K) voltammetric studies have revealed that electrode reactions proceed in a stereoretentive fashion [$E_{\frac{1}{2}}$(*cis*), 0.23 and $E_{\frac{1}{2}}$(*trans*), −0.09 V *vs.* saturated calomel electrode (SCE)] but the species *cis*-$[RuL_2(PPh_3)_2]^+$ and *trans*-$[RuL_2(PPh_3)_2]$ are unstable and spontaneously isomerise affording the stable *trans*-trivalent and *cis*-bivalent complexes respectively, the equilibrium concentration of the unstable isomers being very small. The rates and activation parameters of these isomerisation reactions presumably proceeding by the twist mechanism ($\Delta S^{\ddagger}$ highly negative) have been determined. The factors controlling geometrical preference of oxidation states *viz.*, metal–phosphorus back-bonding and $PPh_3 \cdots PPh_3$ steric repulsion are considered in relation to the osmium analogues reported previously.

This work stems from our interest in the isomer preference of different oxidation states of the same metal ion held in a mixed-donor environment.[1–5] Dithiocarbamate–phosphine complexes of bivalent ruthenium belonging to type **1** have *cis* geometry.[6,7] Nothing is, however, known about their redox behaviour and the effect thereof on co-ordination geometry. This issue is scrutinised in the present work for the case R = Et, R′ = Ph.

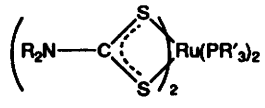

1

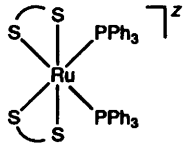

2

2⁺

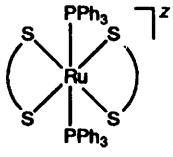

3

3⁺

z
0
+

Results and Discussion

Synthesis and Characterisation.—The species concerning us here are bivalent-*cis*, **2**, trivalent-*cis*, $\mathbf{2}^+$, bivalent-*trans*, **3** and trivalent-*trans*, $\mathbf{3}^+$; of these only **2** and $\mathbf{3}^+$ have been isolated, the latter for the first time, the geometrically unstable species $\mathbf{2}^+$ and **3** could be observed in solution only in voltammetric experiments (see below).

The complex **2** was prepared in nearly quantitative yield from the reaction of equation (1) carried out in boiling ethanol. In

$$[Ru(PPh_3)_3Cl_2] + 2Na[S_2CNEt_2] \longrightarrow \mathbf{2} + PPh_3 + 2\,NaCl \quad (1)$$

earlier preparations hydridophosphine complexes of ruthenium were used as starting materials with much poorer yields.[6,7]

Oxidation of a solution of **2** in dichloromethane–acetonitrile (1:10) solution by aqueous cerium(IV) affords [equation (2)] the blue-green complex $\mathbf{3}^+$ isolated as the PF_6^-

$$\mathbf{2} + Ce^{IV} \longrightarrow \mathbf{3}^+ + Ce^{III} \quad (2)$$

salt in excellent yield. Single crystals could not be prepared for X-ray work but all properties of the complex (see below) are consistent with the *trans* geometry.

Characterisation data for the complexes are set out in Tables 1 and 2. The trivalent complex behaves as a 1:1 electrolyte in MeCN (Λ = 134 Ω^{-1} cm^2 mol^{-1}) and it is paramagnetic corresponding to a t_2^5 ($S = \frac{1}{2}$) configuration (Table 2). Its rhombic EPR spectrum is shown in Fig. 1. Since the symmetry of the co-ordination sphere of $\mathbf{3}^+$ can at best be C_{2h}, the spectrum is indeed expected to be rhombic.

The spectrum was analysed with the help of *g*-tensor theory[8,9] of low-spin d^5 complexes affording axial (Δ) and rhombic (V) parameters as defined in Fig. 1 and listed in Table 2 (some further details are given in the Experimental section). Setting the value of the spin–orbit coupling constant (λ) of ruthenium(III)[10] as 1000 cm^{-1}, we obtain $\Delta \approx 8000$ and $V \approx 1700$ cm^{-1}. The analysis predicts (Table 2) that a pair of ligand-field transitions among the three Kramers doublets should occur near 7000 cm^{-1} (ν_1) and 9000 cm^{-1} (ν_2). The electronic spectrum of the complex shown in Fig. 1 indeed reveals the presence of a relatively weak band at 1550 nm (6450 cm^{-1}) assignable to ν_1. The tail of the relatively strong charge transfer (c.t.) band at 720 nm is believed to obscure the expected ν_2 band.

It is instructive to compare the spectral features of the two

† *Non-SI unit employed:* $\mu_B \approx 9.27 \times 10^{-24}$ J T^{-1}.

Table 1 Analytical[a] and electronic spectral[b] data

Compound	Analysis (%) C	H	N	UV/VIS and NIR λ_{max}/nm (ε/dm^3 mol^{-1} cm^{-1})
cis-[$RuL_2(PPh_3)_2$]	59.85 (59.90)	5.65 (5.60)	2.95 (3.00)	340 (10 000), 255[c] (55 260)
trans-[$RuL_2(PPh_3)_2$]PF_6	51.80 (51.70)	4.70 (4.70)	2.65 (2.60)	1550 (25), 720 (2920), 430[c] (1410), 350[c] (10 420), 310 (19 710)

[a] Calculated values are in parentheses. [b] In dichloromethane at 298 K. [c] Shoulder.

Table 2 Magnetic moments,[a] assignments of EPR *g* values,[b] distortion parameters, and NIR transitions[c] of [$RuL_2(PPh_3)_2$]PF_6

μ_{eff}	1.87
g_x	2.387
g_y	2.311
g_z	1.944
Δ/λ	8.344
V/λ	1.697
ν_1/λ	7.473
ν_2/λ	9.406
ν_1/λ_{obs}[d]	6.452

[a] In the solid state at 298 K. [b] Measurements were made in dichloromethane–toluene (1 : 1) glass at 77 K. [c] Symbols have the same meaning as in the text. [d] Observed frequency converted to ν_1/λ by setting λ = 1000 cm^{-1}.

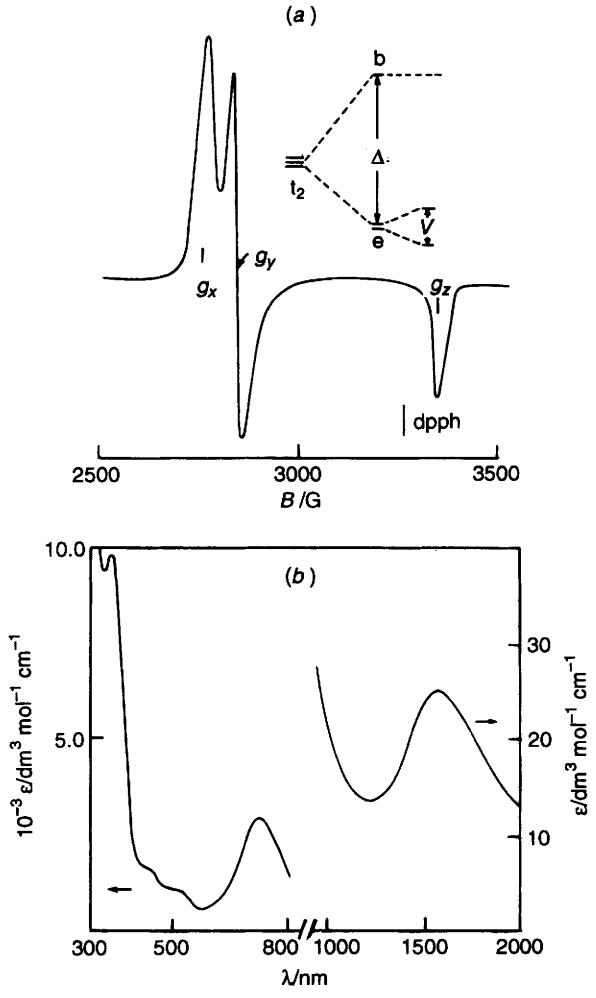

Fig. 1 (*a*) X-band EPR spectrum and t_2 splittings of *trans*-[$RuL_2(PPh_3)_2$]PF_6 in dichloromethane–toluene (1 : 1) glass (77 K); Δ = 8350 cm^{-1}, V = 1700 cm^{-1}. (*b*) Electronic spectrum of *trans*-[$RuL_2(PPh_3)_2$]PF_6 in dichloromethane at 298 K

complexes with those of structurally characterised[11] *cis*-[$OsL_2(PPh_3)_2$] and *trans*-[$OsL_2(PPh_3)_2$]PF_6 (L = S_2CNEt_2). In optical spectra there is a remarkable one-to-one correspondence of bands, both in terms of number and shape; the corresponding energies and intensities being of similar magnitudes. In EPR spectra, the Δ and V parameters (7500 and 1900 cm^{-1} respectively) of the *trans* osmium complex lie close to those (see above) of [$RuL_2(PPh_3)_2$]$^+$. It is clear that the geometrical assignments (*cis* for bivalent and *trans* for trivalent) to the two isolated ruthenium complexes are sound.

Variable-temperature Voltammetry.—Cyclic voltammetry of **2** and **3** have been examined in dichloromethane solution at platinum electrodes over the temperature range 253–303 K. Representative voltammograms are displayed in Fig. 2. The case of **2** will be considered first. Near 300 K one anodic peak A_1 and one cathodic peak C_2, separated from A_1 by $\approx$ 500 mV, are observed. As the temperature is lowered more features become discernible. At 253 K the cathodic peak C_1 corresponding to anodic A_1 becomes clearly observable and the anodic peak A_2 corresponding to cathodic C_2 can be seen in the second and subsequent cycles (Fig. 2).

For **3**$^+$ the voltammogram at 253 K consists of a single quasireversible response with the peaks C_2 and A_2. As the temperature is increased peak A_1 appears and becomes progressively more defined at the expense of A_2. Near 300 K the voltammograms of **2** (initial scan anodic) and **3**$^+$ (initial scan cathodic) are closely alike (Fig. 2).

The above-noted anodic and cathodic peaks can be assigned to the couples of equations (3) and (4). The corresponding $E_{\frac{1}{2}}$

$$A_1, C_1: \mathbf{2}^+ + e \rightleftharpoons \mathbf{2}, \quad E_{\frac{1}{2}}(cis) \qquad (3)$$

$$A_2, C_2: \mathbf{3}^+ + e \rightleftharpoons \mathbf{3}, \quad E_{\frac{1}{2}}(trans) \qquad (4)$$

values are listed in Table 3. In both the couples the stereochemistry is preserved.

However the species **2**$^+$ and **3** are unstable and tend to transform spontaneously to **3**$^+$ and **2** respectively. These transformations become faster as the temperature rises and near 300 K only the anodic response of **2** and the cathodic response of **3**$^+$ remain observable. The voltammetric observations (Fig. 2) are thus consistent with the processes shown in Scheme 1 which is constituted in the couples of equations (3) and (4), and the relevant rate processes (see below).

When **2** is coulometrically oxidised at 0.5 V at room temperature, one electron is quantitatively transferred (Table 3) and the solution is found to contain only **3**$^+$. Similarly room-temperature coulometric reduction of **3**$^+$ at −0.5 V proceeds with the transfer of one electron (Table 3) producing **2** as the only product. The same results are obtained even at low temperature because on the coulometric time-scale the transformations **2**$^+$ ⟶ **3**$^+$ and **3** ⟶ **2** are complete even under these conditions.

The rates of isomerisation steps **3** ⟶ **2** and **2**$^+$ ⟶ **3**$^+$

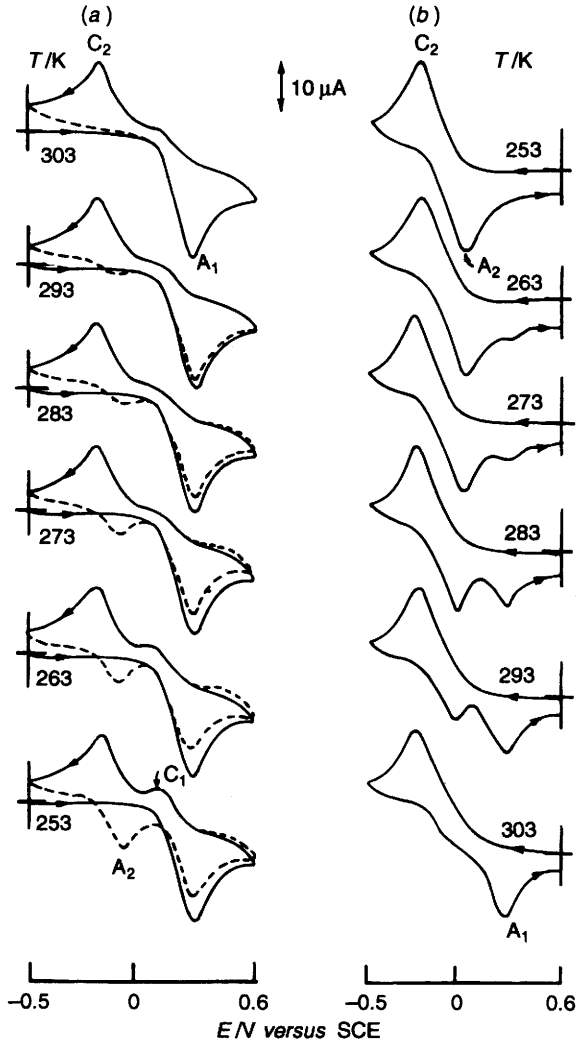

Fig. 2 Variable-temperature cyclic voltammograms (scan rate 50 mV s^{-1}) of 10^{-3} mol dm^{-3} solutions of (*a*) *cis*-$[RuL_2(PPh_3)_2]$ [first cycle (——), second cycle (– – –)] and (*b*) *trans*-$[RuL_2(PPh_3)_2]PF_6$ in dichloromethane

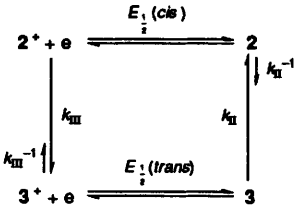

Scheme 1

have been determined by voltammetry at different temperatures.[12] First-order rate constants (k_{II}, k_{III}, Scheme 1) and activation parameters are listed in Table 4. The large entropies of activation are suggestive of the operation of a twist mechanism.[13]

In none of the experiments performed by us we have been able to observe the species **2**$^+$ and **3** in equilibrated solutions. Their equilibrium concentrations are therefore very small, meaning that the rate constants of the backward reactions (k_{II}^{-1} and k_{III}^{-1} in Scheme 1) are small and the equilibrium constants $K_{II} = k_{II}/k_{II}^{-1}$ and $K_{III} = k_{III}/k_{III}^{-1}$ are large ($> 10^2$). The equilibrium constant K_{cr}, equation (5), of the cross-reaction of equation (6) is calculated to be $\approx 10^6$ (Table 3). This is consistent with K_{II}, $K_{III} > 10^2$ since $K_{cr} = K_{II}K_{III}$.

Table 3 Electrochemical[a] and equilibrium data at 253 K

$E_{\frac{1}{2}}(cis)$/V	$E_{\frac{1}{2}}(trans)$/V	n_{ox}[b]	n_{red}[c]	$10^{-6}\,K_{cr}$
0.23	−0.09	1.03	0.96	2.7

[a] Conditions: solvent, dichloromethane; supporting electrolyte, NEt_4ClO_4 (0.1 mol dm^{-3}); working electrode, platinum; reference electrode, saturated calomel electrode (SCE); solute concentration, $\approx 10^{-3}$ mol dm^{-3}, $E_{\frac{1}{2}} = 0.5\,(E_{pa} + E_{pc})$, where E_{pa} and E_{pc} are anodic and cathodic peak potentials, respectively; scan rate, 50 mV s^{-1}. [b] $n_{ox} = Q/Q'$ where Q' is the calculated coulomb count for transfer of one electron and Q is the coulomb count found after exhaustive coulometric oxidation of *cis*-$[RuL_2(PPh_3)_2]$ in dichloromethane (0.1 mol dm^{-3} NEt_4ClO_4). [c] $n_{red} = Q/Q'$ for exhaustive coulometric reduction of *trans*-$[RuL_2(PPh_3)_2]PF_6$.

$$K_{cr} = \exp\{(F/RT)[E_{\frac{1}{2}}(cis) - E_{\frac{1}{2}}(trans)]\} \quad (5)$$

$$2^+ + 3 \rightleftharpoons 2 + 3^+ \quad (6)$$

Comparison with Osmium Analogues.—The stable species are thus **2** and **3**$^+$ and these alone are observable in equilibrated solutions. The species with valence-geometry mismatch, **2**$^+$ and **3**, have been seen only in low-temperature cyclic voltammetric experiments as products of stereoretentive electrode reactions. As in the osmium species,[11] the factors controlling the geometrical preference of oxidation states are (*i*) M–P $n\mathrm{d}_\pi$–$3\mathrm{d}_\pi$ back bonding M^{II} (d^6) ≫ M^{III} (d^5) and *cis* > *trans*, and (*ii*) $PPh_3 \cdots PPh_3$ steric repulsion *cis* > *trans*. The back-bonding advantage in **2** more than offsets the steric disadvantage. In **3**$^+$ the geometry is sterically controlled since back bonding is weak or absent.[14] The trend $E_{\frac{1}{2}}(cis) > E_{\frac{1}{2}}(trans)$ falls in place: the electron ionised belongs to the $4\mathrm{d}(t_2)$ shell which is more stable (back bonding) in the *cis* form. The larger value of K_{Cr} [equation (5)] is another expression of this.

As expected (4d *versus* 5d) the $E_{\frac{1}{2}}$ values for the ruthenium complexes lie at more positive potentials (by ≈150 mV) than those of the osmium analogues[11] and also the rates of isomerisation are much faster (by more than an order of magnitude) in the ruthenium case. One consequence of the latter trend is that the osmium analogue of **3** could be isolated at low temperature and structurally characterised. The back-bonding order $Os^{II} > Ru^{II}$ has a significant effect on K_{II} which is $\approx 10^2$ for Ru^{II} but in the Os^{II} case[11] its value is ≈6 (303 K). In effect the *trans*-osmium(II) complex has better stability than the *trans*-ruthenium(II) analogue.

Conclusion

For $[RuL_2(PPh_3)_2]^z$ the stable valence-geometry combinations are *cis*-bivalent ($z = 0$) and *trans*-trivalent ($z = +$). The latter, isolated as a PF_6^- salt, shows a rhombic EPR spectrum. The species with mismatched *z*-geometry combinations *viz.*, bivalent-*trans* and trivalent-*cis* have been observed in cyclic voltammetry but once formed these isomerise fairly rapidly to the corresponding stable geometries, the equilibrium concentrations of the mismatched species being unobservably small. The observed isomer preference arises from the interplay of back bonding and steric repulsion within the $Ru(PPh_3)_2$ fragment. The present results are qualitatively similar with those of osmium analogues but there are logical quantitative differences in rate and equilibrium constants.

Experimental

Materials.—Commercial ruthenium trichloride was received from Arora Mathey, Calcutta, India and purified by repeated evaporation to dryness with concentrated hydrochloric acid.[15] The compound $[Ru(PPh_3)_3Cl_2]$ was prepared according to the

Table 4 Rate constants and activation parameters in dichloromethane for $[RuL_2(PPh_3)_2]$

trans-$[RuL_2(PPh_3)_2] \longrightarrow$ *cis*-$[RuL_2(PPh_3)_2]$

T/K	$10^2\,k_{II}/s^{-1}$	$\Delta H^{\ddagger}$/kJ mol^{-1}	$\Delta S^{\ddagger}$/J K^{-1} mol^{-1}
273	2.8	52.3 ± 2	−83.4 ± 5
278	4.7		
283	6.5		

cis-$[RuL_2(PPh_3)_2]^+ \longrightarrow$ *trans*-$[RuL_2(PPh_3)_2]^+$

T/K	$10\,k_{III}/s^{-1}$	$\Delta H^{\ddagger}$/kJ mol^{-1}	$\Delta S^{\ddagger}$/J K^{-1} mol^{-1}
258	3.7	48.5 ± 2	−65.2 ± 5
263	6.3		
268	8.9		

reported procedure.[16] Sodium diethyldithiocarbamate was purchased from Aldrich. The preparation of tetraethylammonium perchlorate and the purification of solvents for electrochemical and spectroscopic work were done as before.[15,17] All other chemicals and solvents were of reagent grade and used without further purification.

Physical Measurements.—UV/VIS/NIR spectra were recorded on a Hitachi 330 spectrophotometer. The magnetic susceptibility was measured on a PAR 155 vibrating-sample magnetometer fitted with a Walker Scientific magnet. The X-band EPR spectrum was recorded on a Varian E-109C spectrometer fitted with a quartz Dewar flask for measurements at 77 K (liquid nitrogen) and calibrated with respect to diphenylpicrylhydrazyl (dpph) (g = 2.0037). Electrochemical measurements were done by using a PAR model 370–4 electrochemistry system as described elsewhere.[2a] Compensation for *IR* drop was applied in each case. All experiments were performed under a dinitrogen atmosphere and reported potentials are uncorrected for the junction contribution. Haake model F3K and model D8G digital cryostats and circulators connected to appropriate jacketed cells were used for low-temperature measurements. Solution electrical conductivity was measured using a Philips PR 9500 bridge.

Microanalytical data (C, H, N) were obtained with the use of a Perkin-Elmer model 240C elemental analyser.

Preparation of Complexes.—cis-*Bis(diethyldithiocarbamato)-bis(triphenylphosphine)ruthenium*(II), cis-$[RuL_2(PPh_3)_2]$. To a warm solution of $[Ru(PPh_3)_3Cl_2]$ (100 mg, 0.10 mmol) in ethanol (30 cm^3) was added NaL (40 mg, 0.23 mmol). The mixture was refluxed for 1 h. Upon cooling a bright orange-red microcrystalline solid separated which was collected by filtration, washed thoroughly with water and ethanol, and dried *in vacuo* over P_4O_{10}. Yield 96%.

trans-*Bis(diethyldithiocarbamato)bis(triphenylphosphine)-ruthenium*(III) *hexafluorophosphate*, trans-$[RuL_2(PPh_3)_2]$-PF_6. To a solution of pure *cis*-$[RuL_2(PPh_3)_2]$ (100 mg, 0.11 mmol) in dichloromethane–acetonitrile (1:10, 30 cm^3) was added ammonium cerium(IV) sulfate (100 mg, 0.16 mmol) dissolved in water (5 cm^3). The mixture was stirred magnetically for 15 min during which the solution became deep green-blue. The reaction mixture was then filtered, the filtrate concentrated to 10 cm^3 under reduced pressure, and a saturated aqueous solution of NH_4PF_6 (10 cm^3) added. The deep green crystalline solid thus obtained was collected by filtration, washed with water and dried *in vacuo* over P_4O_{10}, yield 95%.

Treatment of EPR Data.—The procedure used by us for analysing EPR spectra has been detailed elsewhere.[8,14] A very brief outline is given here. The net distortion in the ruthenium(III) *trans* complex, 3^+, can be expressed as the sum of tetragonal (Δ) and rhombic (V) components. Tetragonal distortion (tetragonal axis z) places d_{xy}(b) above d_{xz},d_{yz}(e) [Fig. 1(*a*); here Δ is positive) and rhombic distortion splits the e orbital into non-degenerate components (energy order $d_{yz} > d_{xz}$ where V is positive). Under the combined influence of Δ, V and spin–orbit coupling λ three Kramers doublets are formed representing split components of the octahedral $^2T_2$ term (low-spin t_2^5). Given the signs and magnitudes of g_x, g_y and g_z the values of Δ, V and energies (ν_1 and ν_2) of two ligand-field transitions from ground-to-upper Kramers doublets can be computed. In practice however EPR results provide neither the sign of the three principal g values nor their correspondence to g_x, g_y and g_z. In fact there are eight possible solutions (each representing a cluster of six equivalent solutions). Not all of these are physically meaningful and in most cases one is left to choose one from two alternatives. The correct solution can be chosen confidently when one or both of ν_1 and ν_2 are experimentally observable (as in the present case). The signs of g_x, g_y, g_z, Δ and V in the solution of Table 2 are −, −, +, +, −. In the second solution (not shown in Table 2), the signs are −, −, −, +, − (here the magnitudes of Δ and V are 0.1404 and 0.0287 respectively). The calculated values of ν_1/λ and ν_2/λ in the latter solution are 1.459 and 1.551 respectively, both of which are too small compared to the observed value (6.452) which agrees satisfactorily with the calculated ν_1/λ value, 7.473, of the first solution (Table 2).

Kinetic Measurements.—The rates of conversions $3 \longrightarrow 2$ and $2^+ \longrightarrow 3^+$ were computed from cyclic voltammetric current heights using the method described by Nicholson and Shain[12] for the case of irreversible transformation of electrogenerated species following reversible charge transfer. To apply the method, the couples of the present work are assumed to be reversible although they are only approximately so in practice. In the measurements the variables are temperature (Table 4), scan rate, initial potential and switching potential. The scan rate was varied in the domains 30–50 and 200–400 mV s^{-1} for $3 \longrightarrow 2$ and $2^+ \longrightarrow 3^+$ respectively. In the case of $3 \longrightarrow 2$ the initial potential was set at +0.60 V and the switching potential was varied in the range −0.30 to −0.40 V. For $2^+ \longrightarrow 3^+$ the corresponding values are −0.50 and +0.50 to +0.80 V. The parameters i_{pa}/i_{pc} and τ were determined from the experimental cyclic voltammograms[12] (i_{pa} and i_{pc} are respectively the anodic and cathodic peak heights and τ is the time in s from $E_{\frac{1}{2}}$ to the switching potential). The rate constant (k) was determined in each case from the working curve[12a] of i_{pa}/i_{pc} as a function of $k\tau$. The activation parameters $\Delta H^{\ddagger}$ and $\Delta S^{\ddagger}$ were obtained from the Eyring plot of variable-temperature rate constants.

Acknowledgements

Financial support received from the Council of Scientific and Industrial Research, New Delhi, India is acknowledged. Affiliation with the Jawaharlal Nehru Centre for Advanced Scientific Research, Bangalore, India, is also acknowledged.

References

1 A. Pramanik, N. Bag and A. Chakravorty, *Inorg. Chem.*, 1993, **32**, 811; P. Basu and A. Chakravorty, *Inorg. Chem.*, 1992, **31**, 4980 and refs. therein; P. Basu, S. Bhanja Choudhury, S. Pal and A. Chakravorty, *Inorg. Chem.*, 1989, **28**, 2680.

2 (*a*) A. Pramanik, N. Bag, D. Ray, G. K. Lahiri and A. Chakravorty, *Inorg. Chem.*, 1991, **30**, 410; (*b*) N. Bag, G. K. Lahiri and A. Chakravorty, *J. Chem. Soc., Dalton Trans.*, 1990, 1557.

3 A. Pramanik, N. Bag, D. Ray, G. K. Lahiri and A. Chakravorty, *Inorg. Chem.*, 1991, **30**, 410; A. Pramanik, N. Bag, G. K. Lahiri and

A. Chakravorty, *J. Chem. Soc., Dalton Trans.*, 1992, 101; 1990, 3823.
4 A. M. Bond, R. Colton, J. E. Kevekordes and P. Panagioditou, *Inorg. Chem.*, 1987, **26**, 1430; A. M. Bond, T. W. Hambley, D. R. Mann and M. R. Snow, *Inorg. Chem.*, 1987, **26**, 2257 and refs. therein; B. P. Sullivan and T. J. Meyer, *Inorg. Chem*, 1982, **21**, 1037; D. W. Krassowski, J. H. Nelson, K. R. Brower, D. Hauenstein and R. A. Jackson, *Inorg. Chem.*, 1988, **27**, 4294.
5 D. H. Evans and K. M. O'Connell, in *Electroanalytical Chemistry. A Series of Advances*, ed. A. J. Bard, Marcel Dekker, New York, 1986, vol. 14, p. 113; W. E. Geiger, *Prog. Inorg. Chem.*, 1985, **33**, 275.
6 P. B. Critchlow and S. D. Robinson, *J. Chem. Soc., Dalton Trans.*, 1975, 1367.
7 D. J. Cole-Hamilton and T. A. Stephenson, *J. Chem. Soc., Dalton Trans.*, 1974, 739.
8 G. K. Lahiri, S. Bhattacharya, B. K. Ghosh and A. Chakravorty, *Inorg. Chem.*, 1987, **26**, 4324; S. Bhattacharya and A. Chakravorty, *Proc. Ind. Acad. Sci.*, 1985, **95**, 159; G. K. Lahiri, S. Bhattacharya, M. Mukherjee, A. K. Mukherjee and A. Chakravorty, *Inorg. Chem.*, 1987, **26**, 3359.
9 B. Bleaney and M. C. M. O' Brien, *Proc. Phys. Soc. London, Sect. B*, 1956, **69**, 1216; J. S. Griffith, *The Theory of Transitional Metal Ions*, Cambridge University Press, Cambridge, 1961, p. 364.
10 C. Daul and A. Goursot, *Inorg. Chem.*, 1985, **24**, 3554; N. Bag, G. K. Lahiri, S. Bhattacharya, L. R. Falvello and A. Chakravorty, *Inorg. Chem.*, 1988, **27**, 4396.
11 A. Pramanik, N. Bag and A. Chakravorty, *J. Chem. Soc., Dalton Trans.*, 1993, 237.
12 (*a*) R. S. Nicholson and I. Shain, *Anal. Chem.*, 1964, **36**, 706; (*b*) R. S. Nicholson, *Anal. Chem.*, 1966, **38**, 1406; (*c*) A. N. Singh, R. P. Singh, J. G. Mohanty and A. Chakravorty, *Inorg. Chem.*, 1977, **16**, 2597 and refs. therein.
13 N. Serpone and D. G. Bickley, *Prog. Inorg. Chem.*, 1972, **17**, 391 and refs. therein; D. J. Cole-Hamilton and T. A. Stephenson, *J. Chem. Soc., Dalton Trans.*, 1974, 754.
14 S. Bhattacharya, P. Ghosh and A. Chakravorty, *Inorg. Chem.*, 1985, **24**, 3224.
15 A. R. Chakravarty and A. Chakravorty, *Inorg. Chem.*, 1981, **20**, 275.
16 T. A. Stephenson and G. Wilkinson, *J. Inorg. Nucl. Chem.*, 1966, **28**, 945.
17 A. R. Chakravarty and A. Chakravorty, *J. Chem. Soc., Dalton Trans.*, 1982, 615; S. Bhattacharya and A. Chakravorty, *Proc. Indian Acad. Sci., Chem. Sci.*, 1985, **95**, 159; A. K. Mahapatra, S. Datta, S. Goswami, M. Mukherjee, A. K. Mukherjee and A. Chakravorty, *Inorg. Chem.*, 1986, **25**, 1715.

Received 21*st September* 1994; *Paper* 4/05748A